



Triple-clad photonic lanterns for mode scaling

BIN HUANG,^{1,2,5} JUAN CARLOS ALVARADO ZACARIAS,^{1,2} HUIYUAN LIU,¹
NICOLAS K. FONTAINE,^{1,6} HAOSHUO CHEN,¹ ROLAND RYF,¹ FRANCESCO
POLETTI,³ JOHN R. HAYES,³ JOSE ANTONIO-LOPEZ,² JIAN ZHAO,⁴
RODRIGO AMEZCUA CORREA,² AND GUIFANG LI²

¹Bell Labs, Nokia, 791 Holmdel Rd., Holmdel, NJ 07733, USA

²CREOL, University of Central Florida, Orlando, FL 32816, USA

³Optoelectronics Research Centre, University of Southampton, Southampton, SO17 1BJ, UK

⁴College of Precision Instrument and Opto-Electronic Engineering, Tianjin University, China

⁵binhuang@knights.ucf.edu

⁶nicolas.fontaine@nokia-bell-labs.com

Abstract: We propose a novel triple-clad photonic lanterns for mode scaling. This novel structure alleviates the adiabatic tapering requirement for the fabrication of large photonic lanterns. A 10-mode photonic lantern with insertion losses ranging from 0.6 to 2.0 dB across all the modes and a record-low pairwise 4-dB mode-dependent loss at C-band was demonstrated.

© 2018 Optical Society of America under the terms of the [OSA Open Access Publishing Agreement](#)

OCIS codes: (060.2340) Fiber optics components; (060.2330) Fiber optics communications.

References and links

1. D. J. Richardson, J. M. Fini, and L. E. Nelson, "Space-division multiplexing in optical fibres," *Nat. Photonics* **7**(5), 354–362 (2013).
2. G. Li, N. Bai, N. Zhao, and C. Xia, "Space-division multiplexing: the next frontier in optical communication," *Adv. Opt. Photonics* **6**(4), 413–487 (2014).
3. R. Ryf, H. Chen, N. K. Fontaine, A. M. Velazquez-Benitez, J. Antonio-Lopez, J. C. Alvarado, Z. S. Eznaveh, C. Jin, B. Huang, S. H. Chang, B. Ercan, C. Gonnet, M. Bigot-Astruc, D. Molin, F. Achten, P. Sillard, and R. Amezcua-Correa, "10-Mode Mode-Multiplexed Transmission with Inline Amplification," in 42nd European Conference on Optical Communication (ECOC, 2016), pp. 1–3.
4. G. Labroille, B. Denolle, P. Jian, P. Genevieux, N. Treps, and J.-F. Morizur, "Efficient and mode selective spatial mode multiplexer based on multi-plane light conversion," *Opt. Express* **22**(13), 15599–15607 (2014).
5. B. Huang, C. Xia, G. Matz, N. Bai, and G. Li, "Structured directional coupler pair for multiplexing of degenerate modes," in *Optical Fiber Communication Conference/National Fiber Optic Engineers Conference 2013*, OSA Technical Digest (Optical Society of America, 2013), paper JW2A.25.
6. S. H. Chang, S. R. Moon, H. Chen, R. Ryf, N. K. Fontaine, K. J. Park, K. Kim, and J. K. Lee, "All-fiber 6-mode multiplexers based on fiber mode selective couplers," *Opt. Express* **25**(5), 5734–5741 (2017).
7. K. Takenaga, H. Uemura, Y. Sasaki, S. Nishimoto, T. Uematsu, K. Omichi, R. Goto, S. Matsuo, and K. Saitoh, "Multicore fibre-based mode multiplexer/demultiplexer for three-mode operation of LP01, LP11a, and LP11b," in *2014 The European Conference on Optical Communication* (ECOC, 2014), pp. 1–3.
8. C. Koebele, M. Salsi, D. Sperti, P. Tran, P. Brindel, H. Mardoyan, S. Bigo, A. Boutin, F. Verluise, P. Sillard, M. Astruc, L. Provost, F. Cerou, and G. Charlet, "Two mode transmission at 2×100 Gb/s, over 40 km-long prototype few-mode fiber, using LCOS-based programmable mode multiplexer and demultiplexer," *Opt. Express* **19**(17), 16593–16600 (2011).
9. S. G. Leon-Saval, N. K. Fontaine, J. R. Salazar-Gil, B. Ercan, R. Ryf, and J. Bland-Hawthorn, "Mode-selective photonic lanterns for space-division multiplexing," *Opt. Express* **22**(1), 1036–1044 (2014).
10. B. Huang, N. K. Fontaine, R. Ryf, B. Guan, S. G. Leon-Saval, R. Shubochkin, Y. Sun, R. Lingle, Jr., and G. Li, "All-fiber mode-group-selective photonic lantern using graded-index multimode fibers," *Opt. Express* **23**(1), 224–234 (2015).
11. S. Yerolatsitis, I. Gris-Sánchez, and T. A. Birks, "Adiabatically-tapered fiber mode multiplexers," *Opt. Express* **22**(1), 608–617 (2014).
12. A. M. Velazquez-Benitez, J. C. Alvarado, G. Lopez-Galmiche, J. E. Antonio-Lopez, J. Hernández-Cordero, J. Sanchez-Mondragon, P. Sillard, C. M. Okonkwo, and R. Amezcua-Correa, "Six mode selective fiber optic spatial multiplexer," *Opt. Lett.* **40**(8), 1663–1666 (2015).
13. B. Guan, B. Ercan, N. K. Fontaine, R. P. Scott, and S. J. B. Yoo, "Mode-group-selective photonic lantern based on integrated 3D devices fabricated by ultrafast laser inscription," in *Optical Fiber Communication Conference*, OSA Technical Digest (Optical Society of America, 2015), paper W2A.16.

14. Y. Wu and K. S. Chiang, "Ultra-broadband mode multiplexers based on three-dimensional asymmetric waveguide branches," *Opt. Lett.* **42**(3), 407–410 (2017).
15. N. K. Fontaine, R. Ryf, J. Bland-Hawthorn, and S. G. Leon-Saval, "Geometric requirements for photonic lanterns in space division multiplexing," *Opt. Express* **20**(24), 27123–27132 (2012).
16. A. M. Velazquez-Benitez, J. E. Antonio-Lopez, J. C. Alvarado-Zacarias, G. Lopez-Galmiche, P. Sillard, D. Van Ras, C. Okonkwo, H. Chen, R. Ryf, N. K. Fontaine, and R. Amezcua-Correa, "Scaling the fabrication of higher order photonic lanterns using microstructured preforms," in *ECOC 2015* (2015), pp. 1–3.
17. B. Huang, J. C. Alvarado-Zacarias, N. K. Fontaine, H. Chen, R. Ryf, F. Poletti, J. R. Hayes, J. E. Antonio-Lopez, R. Amezcua-Correa, and G. Li, "10-Mode Photonic Lanterns Using Low-Index Micro-Structured Drilling Preforms," in *Optical Fiber Communication Conference, OSA Technical Digest* (Optical Society of America, 2017), paper Tu3J.5.
18. N. K. Fontaine, R. Ryf, M. A. Mestre, B. Guan, X. Palou, S. Randel, Y. Sun, L. Gruner-Nielsen, R. V. Jensen, and R. Lingle, "Characterization of Space-Division Multiplexing Systems using a Swept-Wavelength Interferometer," in *OFC 2013* (2013), paper OW1K.2.
19. B. Huang, H. Chen, N. K. Fontaine, C. Jin, K. Shang, R. Ryf, R.-J. Essiambre, Y. Massaddeq, S. LaRochelle, and G. Li, "Spatially and Spectrally Resolved Gain Characterization of Space-Division Multiplexing Amplifiers With Coherent Swept-Wavelength Reflectometry," *J. Lightwave Technol.* **35**(4), 741–747 (2017).

1. Introduction

Space-division multiplexing (SDM) is viewed as a promising way to overcome the capacity crunch of single-mode fibers (SMFs) [1, 2]. SDM in few-mode fibers (FMF) or multi-mode fibers (MMF) utilizes multiple spatial channels to increase capacity per fiber. Recently, SDM transmission in a 10-spatial mode graded-index (GI) FMF with inline amplification was demonstrated for a distance of 121 km [3]. Spatial multiplexers for mode (de)multiplexing are key components for SDM. Various spatial multiplexers have been proposed, such as multi-plane mode converters [4], directional couplers [5–7] and free space converters [8]. Among all the candidates, photonic lanterns (PLs) [9–14] are very promising because they offer low insertion loss (IL), low mode-dependent loss (MDL), scalability and compactness. The fiber-based PL forms a low-loss interface between a MMF or FMF, and a set of SMFs, which enables mapping from fundamental modes of SMFs to spatial modes of a MMF. When the number of modes of the PL scales up, the IL and MDL deteriorate dramatically. A 10-mode PL fabricated recently had an IL ranging between 0.7 dB and 3.2 dB when spliced to the 10 mode fiber, and a pairwise MDL of 8.7 dB [3]. To achieve better performance, two obstacles need to be overcome. One is fabrication complexity; it is difficult, especially manually, to position a set of input SMFs or FMFs into the fluorine tubes while maintaining precise geometry [15]. The use of stack-and-draw preforms can greatly ease the fabrication process [16], but such preforms would inevitably add more cladding material, which makes the second obstacle even more challenging. The second obstacle is the adiabatic tapering requirement as the mode number scales up. It can be estimated, from cladding-area considerations, that the required tapering length increases as N^2 for a total of N modes [11]. The stack-and-draw method adds extra cladding material, further exacerbating the adiabatic tapering requirement.

In this paper, we demonstrate PLs using novel triple-clad micro-structured preforms fabricated by drilling, which not only ease the fabrication complexity for mode scalability but also alleviate the adiabatic requirement for lantern tapering [17]. In addition, the guiding region at the end of the photonic is circular, which leads to low losses when spliced to the 10 mode transmission fiber. For a 10-mode (per polarization) PL fabricated using the proposed method, the IL ranges from 0.6 to 2.0 dB across all the modes when spliced to a 10-mode GI fiber. The pair-wise MDL reaches a record low level of 4 dB.

2. Rationale

The adiabaticity requirement for two modes E_1 and E_2 not to couple to each other during tapering is:

$$\left| \frac{2\pi}{\beta_1 - \beta_2} \frac{d\rho}{dz} \int E_1 \frac{\partial E_2}{\partial \rho} dx dy \right| \ll 1 \quad (1)$$

where β_1 and β_2 are the propagation constants of the modes E_1 and E_2 . ρ is the local core radius, z is the longitudinal distance along the PL. The term $\partial E / \partial \rho$ is the rate of change of the mode field and $d\rho / dz$ is the tapering rate. It can be seen that if the rate of change of the mode field small, the adiabatic requirement can be more easily met. Previous methods to maintain the adiabatic requirement includes the use of reduced-cladding fibers [11] and GI multimode fibers [10].

Figure 1 shows the double-clad PL facet before tapering used to date (a), and the proposed triple-clad PL facet (b). In both figures, the input fibers [Ge-doped graded-index core (black) and pure-silica cladding (dark blue)], three of them residing on a small circle and the other seven residing on a large circle, are identical for these two preforms. The input fibers simulated are commercial 10 mode graded-index fiber. For double-clad PL, which is widely used in fabrication [9–12], it has an outer cladding which is heavily F-doped with a refractive index of 1.430 and the second cladding layer (inner cladding of the preform plus the cladding of the input fiber) which is pure silica with index 1.444 shown in Fig. 1(a). For our proposed triple-clad PL in Fig. 1(b), the inner cladding of the preform is lightly F-doped with a refractive index of 1.442, lower than the pure-silica cladding of the input fiber, but higher than the outer cladding, thus forming a triple-clad structure. The difference between these two preforms seems to be small but they actually lead to very different behaviors in mode evolution for these two structures when they are tapered down in fabrication. The reason is as follows. When the preform is tapered down, the fundamental mode supported in each input fiber core will become less guided and expand. This expansion in the double-clad structure remains unimpeded until the outer cladding. On the other hand, when the proposed triple-clad preform is tapered down, the lower-index inner cladding suppresses mode expansion.

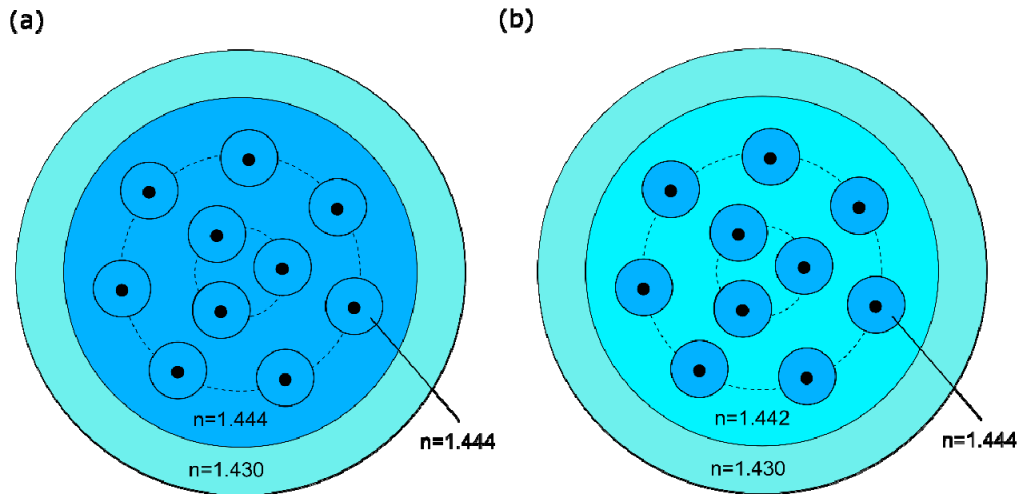


Fig. 1. Micro-structured preform with (a) double-clad PL (b) triple clad PL

To show these evolution behaviors quantitatively, we used the geometries in Figs. 2(a) and 2(b) to perform a simplified simulation of mode evolution comparison with one fiber case, while the physics remains the same as in Fig. 1. Figure 2(a) is in principle one core double-clad PL and Fig. 2(b) is one core triple-clad PL. For both cases in Fig. 2, the input cores are the same graded-index core, which has been shown to be more advantageous during tapering than step-index core [10]. We then calculate the mode profiles of the fundamental mode (lowest order mode) of the both structures at different tapering ratios. Figure 2(c) shows

the mode-field diameter (MFD) of the fundamental mode versus the taper ratio (from 1 to 0.03). The MFD of both cases initially decreases at the same rate until the taper ratio around 0.3, after which the MFD starts to increase. However, the rate of the increase of the MFD for the double-clad structure in Fig. 2(a) is five times larger than that for the triple-clad structure in Fig. 2(b), which demonstrates that our proposed structure is more adiabatic during tapering.

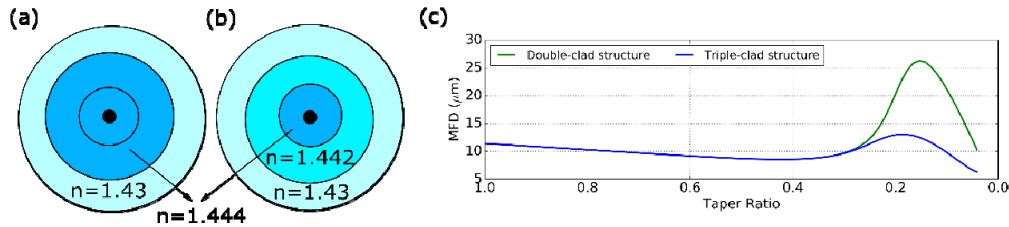


Fig. 2. Schematic of simplified double-clad (a) and triple-clad (b) structures, and the mode field diameters of the fundamental mode of the structures in (a) and (b) vs the taper ratio.

Also, based on simulations using the beam propagation method, we further prove the validity of our proposed structure by calculating the MDLs and ILs of the PLs using the two preforms in Figs. 1 (a) and 1(b). The total length of the PLs in the simulations is 5 cm and the linear taper ratio is 1/36. The IL is calculated to be 0.01dB and the MDL is 0.03 dB for the novel triple-clad structure. As expected, the double-clad preform results in an IL of 0.23 dB and a MDL of 0.7 dB, both at least one order of magnitude larger.

3. Fabrication

The proposed preform was fabricated in several steps. First, we fabricated the lightly F-doped inner cladding and inserted 10 identical GI 10-mode commercial fibers into the drilled holes. The facet is same to the structure shown in Fig. 1(b) except we do not have the lower index outer layer (light blue). The size of the structure is as follows. Ten drilled holes with a diameter of $130\ \mu\text{m}$ were arranged in two circles. Three holes were drilled in the small circle of diameter $203\ \mu\text{m}$ while seven holes were drilled in the larger circle of diameter $528\ \mu\text{m}$. The outer diameter of the inner cladding is $780\ \mu\text{m}$. However, the heavily F-doped tube shown in the middle of Fig. 3 which should act as an outer layer has a smaller diameter than $780\ \mu\text{m}$. It has inner diameter of only around $350\ \mu\text{m}$, so we cannot insert the inner cladding directly into the heavily-doped outer layer. We tapered the inner cladding with the input fibers by the ratio of 1/2.4 shown in the left of Fig. 3. After that, we inserted the tapered inner cladding into the outer cladding. One thing to note that at this taper ratio, the fundamental mode of the input fiber was still well confined in each individual core. In the final step, the entire preform was tapered by a ratio of 1/16 as shown in the right of Fig. 3. The tapering length of the PL is about 5cm and the final core diameter is around $20\ \mu\text{m}$ with cladding size slightly less than $90\ \mu\text{m}$. The PL was then cleaved and spliced to a GI 10-mode commercial fiber.

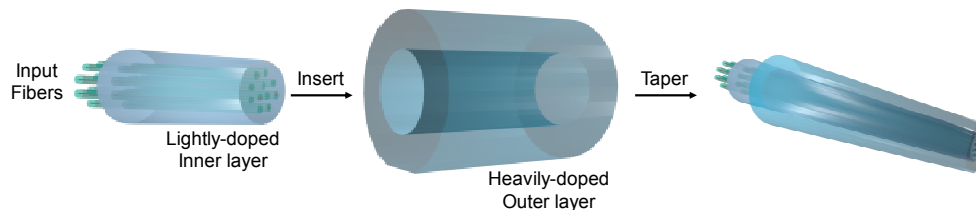


Fig. 3. Schematic of the photonic lantern fabrication process.

4. Characterization

The output intensity profiles of the PL before and after splicing to a 10-mode GI-FMF are shown in Figs. 4 and 5. The first three output intensity profiles in Fig. 4 come from the inner ring the others from the outer ring. The PL is not designed to be mode-selective, however, certain level of mode selectivity is observed. The modal content of the first three output constitutes a large portion of LP_{01} and LP_{11} . We believe the whole geometric structure and the small core to core distance within the inner ring play a big role. The exact modal content depends on various factors, distance between claddings, distance between inner ring and outer ring, the location of cores of inner ring and outer ring and so on. It is also possible if we want to make mode selective lanterns using this structure. It can be achieved by using different cladding refractive index and proper cladding size and spacing.

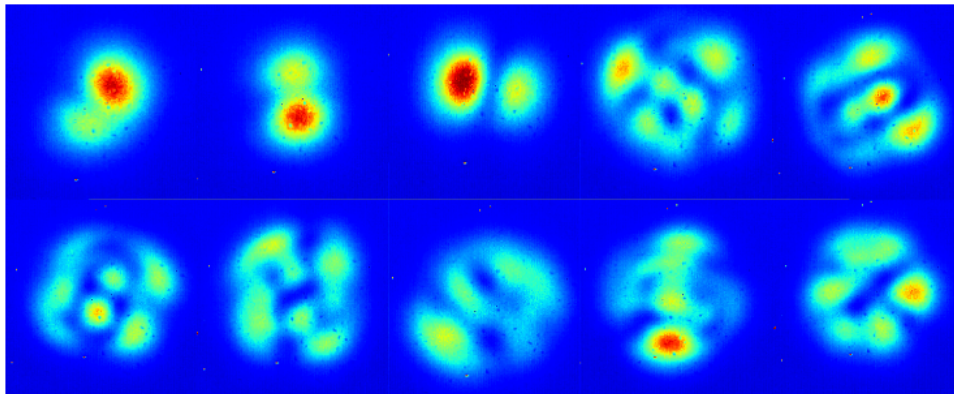


Fig. 4. Output intensity profiles of photonic lantern corresponding to the 10 input fibers.

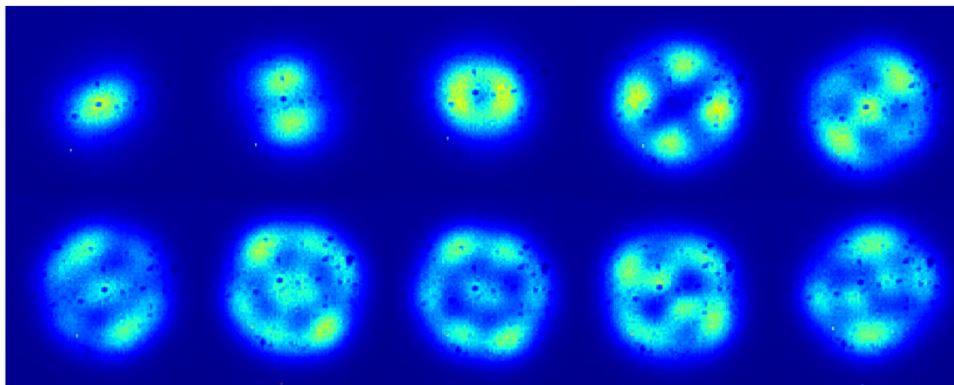


Fig. 5. Output intensity profiles of photonic lantern corresponding to the 10 input fibers after being spliced to a 10 mode GI fiber.

Next, we characterize the insertion loss and mode-dependent loss of the 10-mode PL. The ILs corresponding to the ten input fibers were measured to be from 0.6 dB to 2 dB. To obtain MDL, the full amplitude and phase transfer matrix must be measured. The setup for the characterization of the back-to-back transfer matrix of the 10-mode PL is shown in Fig. 6 which includes a swept-wavelength interferometer (SWI). The SWI comprises a tunable laser source, a polarization multiplexer (Pol. Mux), a fiber interferometer and a polarization-diversity coherent receiver. The receiver includes one polarization beam splitter (PBS), two 2 x 2 couplers, two balanced photodiodes and two 100-MS/s analog-to-digital converters. In the

experiment, light coming from the swept-wavelength laser source is split into two branches, the signal and the reference. In the signal branch, a polarization multiplexer ensures that two orthogonal polarizations are launched with same power. Fiber delays were added at the input and output of the signal to differentiate the input-output response in the time domain. The swept-wavelength signal goes through one fiber delay bank into the PL, and gets reflected by a mirror. Then it goes through the PL from the opposite side, enters the other delay bank and finally into the receiver. In this arrangement, light goes through the PL twice, yielding the pair-wise MDL of the PL in the back-to-back configuration.

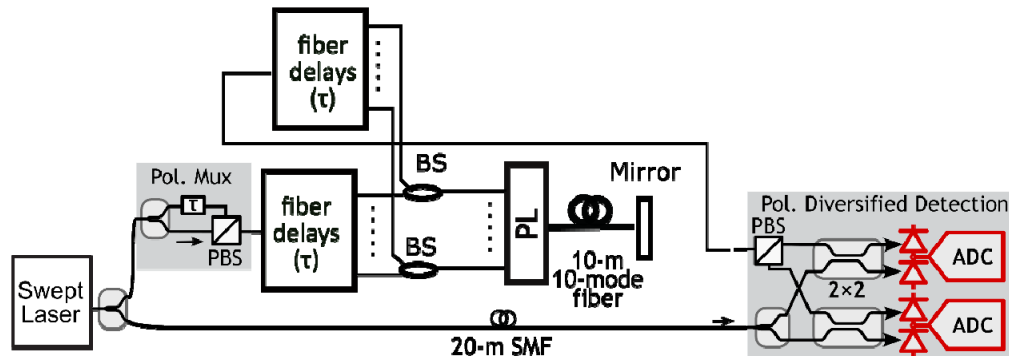


Fig. 6. Experimental setup for the transfer matrix measurement.

The full 20×20 complex transfer matrix at each wavelength can be obtained as shown in [18,19]. The MDL was then calculated by using singular-value decomposition (SVD) of the transfer matrix at each wavelength. The MDL for the pair of identical PLs over the entire C band (191.45 – 195.85 THz) is less than 4.5 dB, as shown in Fig. 7, corresponding to a 2 dB MDL at C band for each.

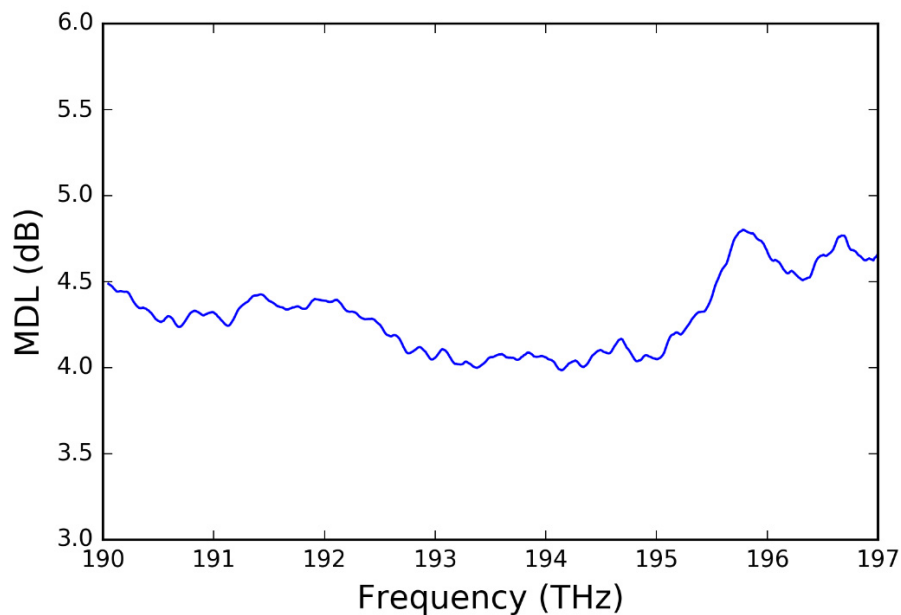


Fig. 7. MDL vs frequency

5. Conclusion

We demonstrate a 10-mode triple-clad PL with low IL and MDL. This triple-clad structure is proven to be better than previous fabricated PL in terms of adiabatic requirement, thus the mode scaling ability.

Funding

This work was supported by the ICT R&D program of MSIP/IITP, Republic of Korea. [R0101-16-0071, Research of mode-division-multiplexing optical transmission technology over 10 km multi-mode fiber].